

# Emergence of spatial structure in the tumor microenvironment due to the Warburg effect

Carlos Carmona-Fontaine<sup>a,1</sup>, Vanni Bucci<sup>a</sup>, Leila Akkari<sup>b</sup>, Maxime Deforet<sup>a</sup>, Johanna A. Joyce<sup>b</sup>, and Joao B. Xavier<sup>a,1</sup>

<sup>a</sup>Computational Biology Program, <sup>b</sup>Cancer Biology and Genetics Program, Memorial Sloan-Kettering Cancer Center, New York, NY 10065

Edited by Robert H. Austin, Princeton University, Princeton, NJ, and approved October 15, 2013 (received for review June 25, 2013)

Drastic metabolic alterations, such as the Warburg effect, are found in most if not all types of malignant tumors. Emerging evidence shows that cancer cells benefit from these alterations, but little is known about how they affect noncancerous stromal cells within the tumor microenvironment. Here we show that cancer cells are better adapted to metabolic changes in the microenvironment, leading to the emergence of spatial structure. A clear example of tumor spatial structure is the localization of tumor-associated macrophages (TAMs), one of the most common stromal cell types found in tumors. TAMs are enriched in well-perfused areas, such as perivascular and cortical regions, where they are known to potentiate tumor growth and invasion. However, the mechanisms of TAM localization are not completely understood. Computational modeling predicts that gradients—of nutrients, gases, and metabolic by-products such as lactate—emerge due to altered cell metabolism within poorly perfused tumors, creating ischemic regions of the tumor microenvironment where TAMs struggle to survive. We tested our modeling prediction in a coculture system that mimics the tumor microenvironment. Using this experimental approach, we showed that a combination of metabolite gradients and differential sensitivity to lactic acid is sufficient for the emergence of macrophage localization patterns *in vitro*. This suggests that cancer metabolic changes create a microenvironment where tumor cells thrive over other cells. Understanding differences in tumor-stroma sensitivity to these alterations may open therapeutic avenues against cancer.

tumor adaptation | mathematical model | image analysis

Cancer cells in tumors display pronounced metabolic alterations (1–10). The genetic and biochemical mechanisms behind these changes are under intensive investigation, but the question of how metabolic changes affect noncancerous cells in the tumor microenvironment remains largely unanswered. The Warburg effect—or oxidative glycolysis, a process whereby cells exhibit a high glycolytic rate even in the presence of oxygen—is arguably the best-known metabolic alteration in cancer (1). Due to a lower yield of glucose to ATP associated with glycolysis, the Warburg effect was initially viewed as a detrimental aberration (1, 5). However, it is now clear that ATP is not a limiting resource for cell growth (4, 9) and that glycolytic alterations increase glucose and glutamine uptake, enhance reductive power, and favor anabolism by retaining carbon-rich macromolecules (4, 7, 9). Thus, rather than being detrimental, metabolic alterations in tumor cells can be required to sustain the high proliferation rate that characterizes malignant cancers (4, 7, 9). In fact, similar metabolic changes occur in healthy processes with rapid population growth such as pluripotent stem-cell proliferation (11), T-cell activation (12), embryonic development (13), and wound healing (14), suggesting that cancer cells have co-opted conserved metabolic processes used by rapidly proliferating cells (4, 7, 9).

Despite their beneficial effect for cell proliferation, metabolic changes have dramatic consequences on the extracellular milieu. Alterations in tumor metabolism were first identified by studying how cancer cells alter their culture media (1, 5). Chaotic vascularization can be a feature in tumors *in vivo*, which intensifies

the effect of cancer cells on their microenvironment and causes damaging processes such as acidosis, hypoxia, and nutrient deprivation (15, 16). Thus, cancer cells must balance the benefits of an altered metabolism with its potentially toxic extracellular consequences.

Cancer is a disease of clonal evolution where different cell lineages compete (17, 18). Mathematical models in the literature suggest that metabolic modifications can be advantageous for lineages competing within tumors (16, 19–21). Nonetheless, how stromal cells within tumors cope with these changes has been largely neglected. Thus, it is possible that a toxic microenvironment created by metabolic alterations may be a mechanism for cancer cells to gain a selective advantage.

We focused our study on how tumor metabolism affects macrophages. Tumor-associated macrophages (TAMs) are one of the most common stromal cell types found within tumors, and their number is directly correlated with poor patient prognosis in the majority of cancers analyzed to date (22–26). TAMs are well adapted to, and recruited toward, low-oxygen-tension regions (22, 27, 28). However, TAMs *in vivo* are also enriched in well-perfused regions of the tumor—such as the invasive edge and perivascular areas—where they potentiate cancer progression and invasion (29–31). Other tumor-associated stromal cells, live, or even dying cancer cells are known to recruit macrophages to the tumor (32–34). Nonetheless, why resident and recruited macrophages do not infiltrate the tumor homogeneously remains poorly understood. An intriguing hypothesis then is that TAMs may be precluded from poorly perfused regions because metabolic alterations generate a toxic environment where only adapted tumor cells can survive.

## Significance

Cancer cells undergo dramatic metabolic alterations, such as the Warburg effect where glucose is consumed independently of oxygen, leading to high lactic acid production. Although these alterations can give growth advantages to cancer cells, they have a profound effect in the extracellular environment, and thus it is not clear how they affect healthy cells. Here we show that lactic acid accumulation can impair the survival of tumor-associated macrophages. Using a multidisciplinary combination of computational and experimental methods, we show that this decreased survival can lead to spatial patterns of macrophage localization that resemble how tumor-associated macrophages distribute in real tumors. Spatial patterns can potentiate tumor growth, and thus understanding how they are formed may bring therapeutic insights.

Author contributions: C.C.-F., J.A.J., and J.B.X. designed research; C.C.-F., V.B., L.A., and M.D. performed research; C.C.-F., V.B., L.A., M.D., J.A.J., and J.B.X. contributed new reagents/analytic tools; C.C.-F., V.B., L.A., M.D., and J.B.X. analyzed data; and C.C.-F., J.A.J., and J.B.X. wrote the paper.

The authors declare no conflict of interest.

This article is a PNAS Direct Submission.

<sup>1</sup>To whom correspondence may be addressed. E-mail: carmonac@mskcc.org or xavierj@mskcc.org.

This article contains supporting information online at [www.pnas.org/lookup/suppl/doi:10.1073/pnas.1311939110/-DCSupplemental](http://www.pnas.org/lookup/suppl/doi:10.1073/pnas.1311939110/-DCSupplemental).

Here we show that metabolically altered microenvironments can indeed provide cancer cells with a selective advantage. In particular, these cancer cells are more resistant than macrophages to high levels of lactic acid produced by their glycolytic metabolism. We combine computational modeling with a custom-made cell culture system that allows the emergence of spatially graded microenvironments ranging from well-perfused to ischemic regions. With this approach we show that differential sensitivity to lactic acid between cancer cells and macrophages is sufficient to generate localization patterns that resemble *in vivo* observations.

## Results

**Glycolytic Cancer Cells Are Adapted to Lactic Acid.** We first investigated the impact of the metabolic activity of cancer and stromal cells on their surrounding microenvironment. We used primary bone marrow-derived macrophages (BMDMs) as our model for stromal cells and MTLn3 cells, an aggressive metastatic breast adenocarcinoma line widely used in tumor-stromal studies (35), as a model cancer cell line. When grown for 24 h, MTLn3 cells, but not macrophages, significantly increased lactate levels and decreased glucose levels in the culture media even in the presence of oxygen, evidencing enhanced oxidative glycolysis [Fig. 1*A*; note that these trends are maintained when metabolites levels are normalized by total biomass (*SI Appendix, Fig. S1A*)]. In addition, MTLn3 cancer cells showed higher glutamine consumption, as has been reported for other cancer cells (36), whereas other measured metabolites were not substantially changed (*SI Appendix, Fig. S1A*). We confirmed these observations by measuring glucose consumption and lactate production in a panel of cancerous and noncancerous cells. All tested cancer cells showed a similar behavior to MTLn3, whereas low passage, nontransformed, mouse embryonic fibroblasts (MEFs) behaved similarly to macrophages (*SI Appendix, Fig. S1B*). These data confirm that at least a panel of cancer cells, but not stromal cells, display typical metabolic alterations such as the Warburg effect.

Next, we examined how MTLn3 cells and macrophages adapt to nutrient depletion. We examined the role of starvation by

culturing cells for 24 or 48 h under a range of nutrient compositions and measuring cell viability. Most viability methods rely on measuring activity of metabolic enzymes at a population level, which may be altered by nutrient limitation and produce experimental biases. We circumvented this limitation by adding a fluorescent dye that is incorporated only by cells with compromised cell membranes. This allowed us to measure viability at the single-cell level using microscopy and image analysis (*SI Appendix*). Starvation by the withdrawal of glucose, glutamine, or serum did not have a significantly different effect on the survival of either cell type (*SI Appendix, Fig. S2A*). Likewise, hypoxia, *i.e.*, oxygen starvation alone or combined with different nutrient deprivations, did not induce notable differential changes in the viability of the cells (*SI Appendix, Fig. S2A*). The observation that macrophages remain viable under oxygen deprivation is consistent with reports of macrophages being recruited to anoxic and necrotic regions of tumors (28) and the observation that macrophages survive and adapt well to hypoxia (27). In summary, nutrient deprivation and hypoxia appear to affect MTLn3 cells and macrophages equivalently.

Next we investigated the effect of lactate on cell viability, because its secretion levels are remarkably different among tested cancerous and noncancerous cell lines. Adding lactic acid to the growth media showed that, although extremely high levels of lactic acid are lethal for both MTLn3 and macrophages, MTLn3 cells survive better than macrophages at intermediate levels (~25–30 mM; Fig. 1*B*). These levels of lactic acid are close to the ones produced by MTLn3 cells (Fig. 1*A*) and to those reported in human tumors (37, 38). Control experiments carried out using sodium lactate instead of lactic acid did not show a significant difference in survival, suggesting that the detrimental effect of lactic acid to macrophages is through media acidification (*SI Appendix, Fig. S2B*). Additional experiments with our cell panel using lactic acid confirmed that cancerous cell lines tend to be more resistance to lactic acid than macrophages and MEFs (*SI Appendix, Fig. S2C*). Furthermore, MTLn3 cells are also more resistant than macrophages to acetic acid, supporting the role of pH in cell viability (*SI Appendix, Fig. S2D*).

To evaluate whether this differential effect still occurs when the two cell types share the same microenvironment, we cocultured MTLn3 and macrophages at a range of lactic acid concentrations and measured the relative contribution of each cell type to the final population after 24 h. Lactic acid specifically reduced the proportion of macrophages in the coculture population (Fig. 1*C*), confirming that MTLn3 cells are fitter when lactic acid accumulates. This effect can be reverted by the addition of bicarbonate to the media, further confirming the role of pH (*SI Appendix, Fig. S3 C and D*).

**Model Reveals That Restricted Perfusion Generates Metabolic Gradients and Spatial Structure in Cell Populations.** TAMs *in vivo* are enriched in well-perfused regions of large tumors such as in perivascular regions and at the invasive edge (Fig. 2*A* and *SI Appendix, Fig. S4*). However, in small tumors TAMs are usually dispersed throughout the tumor mass (30) (*SI Appendix, Fig. S4*). The differential sensitivity shown in our experiments suggests that macrophages may not survive in conditions of high lactic acid concentration, which is more likely to occur in larger, poorly perfused, tumors (16). We therefore asked whether the accumulation of lactic acid in poorly perfused regions is sufficient to explain the localization patterns of macrophages. Computational models have shown that glycolysis would lead to lactate gradients due to increased secretion and to steep drops in pH (16, 19), but the effect of these gradients on stromal cells remains unexplored. Thus, we created a computational model where a mixed population of tumor cells and macrophages coexist in a confined space representing tissue adjacent to a blood capillary or at the tumor edge next to normal tissue (Fig. 2*B*). In this model, cells consume resources (*e.g.*, glucose and oxygen, denoted as “R” in Fig. 2*B*) at rate  $q$  and secrete metabolic waste products (such as lactic acid, denoted as “W” in Fig. 2*B*) at rate  $k$ . Resources

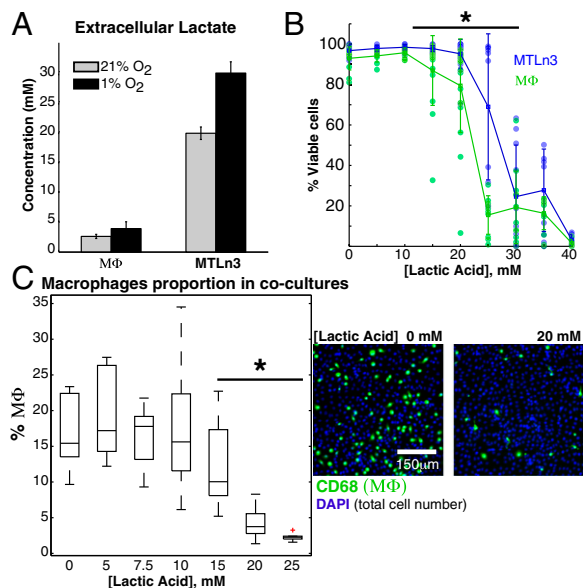


**Fig. 1.** Cancer cells are adapted to toxic environments produced by the Warburg effect. (*A*) MTLn3 breast cancer cells but not macrophages (MΦ) display the Warburg effect. (*B*) Macrophages are more sensitive to lactic acid that lowers media pH. (*C*) Boxplots showing the effect of lactic acid on in cocultures. The red plus sign (+) denotes outliers. (*Right*) Representative examples. Error bars in *A* and *B* represent SD from the mean obtained in at least three triplicated experiments. Data points are always obtained from independent visual fields. \* $P < 0.05$ .

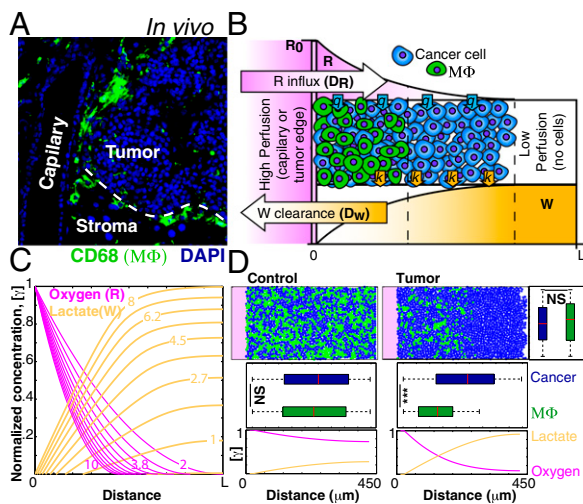


**Fig. 2.** Mathematical model predicts that differential sensitivity to waste products (W), such as lactic acid, leads to spatial structure. (A) TAMs (MΦ) in vivo show spatial patterns of localization, with enrichment at the invasive edge and in perivascular areas. Representative image of macrophage staining (CD68, green) of a pancreatic islet tumor in the RT2 model. (B) Schematic representation of the mathematical model. (C) Concentration profiles of resources and waste products calculated with different parameters (indicated by the numbers over the lines) in the combined analytical model. (D) (Upper) Agent-based simulation showing the distribution of particles representing macrophages (green) and cancer cells (blue). (Lower) Oxygen/lactate profiles. Note that if oxygen diffusion is increased by 10x, gradients are shallow and no spatial structure emerges. Boxplots show the distribution of centroids across the two axes. \*\*\* $P < 0.001$ ; NS, not significant.

diffuse into the system from one side (with diffusivity  $D_R$ ). Similarly, waste is cleared via the same side with diffusivity  $D_W$ . In our experiments, cancer cells and macrophages are equally resistant to starvation and hypoxia (*SI Appendix, Fig. S24*), but macrophages are more sensitive to lactic acid levels (Fig. 1 B and C). Because lactic acid production increases in low oxygen (Fig. 1A), hypoxia could lead to macrophage death indirectly due to lactic acid accumulation. Thus, in our model the levels of waste (lactic acid) are a function of resource (oxygen) depletion (*SI Appendix, Table S1*).

Solving the model analytically gives the expected decreasing curve for R and increasing levels of W (Fig. 2C). Using this model, and incorporating biophysically relevant parameters (*SI Appendix, Table S2*), we simulated the evolution of a cell coculture using an agent-based computational approach. We adopted an established off-lattice agent-based modeling (ABM) framework used to model other complex multicell systems such as bacterial biofilms (39, 40). Similar approaches have been used to model tumor growth (20, 41). In this ABM framework, cells are modeled as discrete agents with rules that mimic the behavior of cells (growth, division, death, etc.), whereas gradients of metabolites are modeled using continuum partial differential equations (*SI Appendix*) (39). Under these conditions, the simulated cancer cells and macrophages coexist in well-perfused regions, but only cancer cells are able to survive in ischemic regions (Fig. 2D, “Tumor”; *SI Appendix, Movie S1*). In contrast, when we conduct the simulations making oxygen 10 times more diffusive to increase perfusion, the spatial structure is lost (Fig. 2D, “Control”; *SI Appendix, Movie S1*). Thus, spatial structure can be an emergent property if cells have different sensitivities to microenvironmental conditions when perfusion is poor. Importantly, in our simulations, spatial heterogeneities are not externally imposed but are the result of diffusion and reaction processes. Similar models have been used to explain the formation of necrotic cores (42) or the evolution of more aggressive tumor clones (16, 19, 20). Here, our model shows that self-generated gradients can play an

important role in the spatial distribution of cancer cells and tumor-associated macrophages resembling in vivo observations.

**Experimental Validation with a Tissue Mimetic System.** Computational model predictions can be compared with in vivo data, such as imaging (43, 44), but models are difficult to test experimentally. In vivo manipulations are technically challenging and in vitro models often neglect important features such as spatial structure. To circumvent these limitations, we adapted a tissue-mimetic culture system (45) to mimic the tumor microenvironment in vitro. This setup allows coculture of different cell types and the spontaneous formation of gradients while still permitting direct cell imaging (Fig. 3A and *SI Appendix*). Briefly, cells are cultured in a small volume (in the  $\sim 50\text{-}\mu\text{L}$  internal chamber) that is connected to a larger volume (the  $\sim 2\text{-mL}$  external chamber) through a small slit or opening ( $\sim 0.3\text{ mm}$  wide). The external chamber thus constitutes a bulk source of nutrients and provides a sink of waste products, creating a directional gradient of any diffusible substances consumed or produced by cells in the internal chamber. The self-generated gradients in this simple setup ensure that cells proximal to the slit will be well perfused, whereas cells distal to the slit will be progressively more ischemic (Fig. 3A). The cell population cultured in the interior chamber is imaged using a programmable motorized microscope stage and tiled microscopy to build large-scale mosaics of adjacent pictures, producing images that combine high resolution with a wide field of view. Thus, we can investigate cell populations at multiple scales from the single-cell to multicellular level simultaneously (Fig. 3A and B; *SI Appendix, Fig. S5A*).

We first confirmed that our system allows the spontaneous formation of metabolite gradients. We used a glioma cell line (C6-HRE-GFP) that expresses GFP under hypoxic conditions

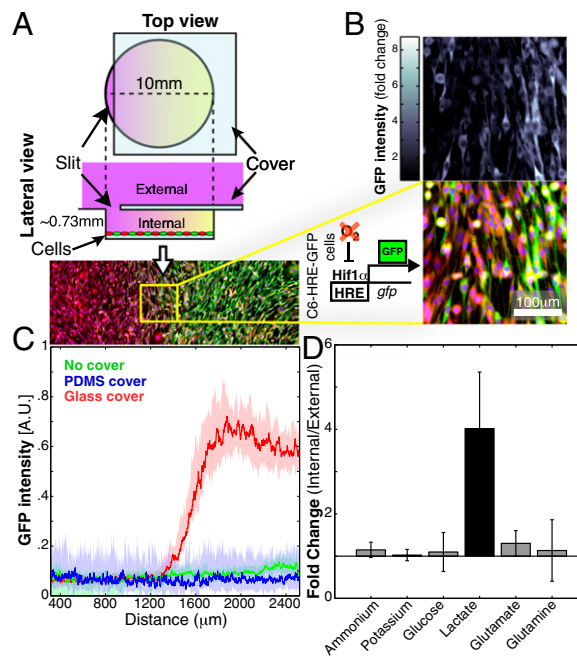


**Fig. 3.** Experimental culture system that mimics the tumor microenvironment. (A) Schematic representation of the culture system scanned using tiling microscopy. (B) C6-HRE-GFP cells showing GFP (green) expression and a cell membrane stain (CMPTX, Molecular Probes). (Upper) GFP/CMPTX ratios (in grayscale) used for quantification. (C) Quantification of GFP signal shows that oxygen gradients emerge in chambers with glass covers but not in control or PDMS-covered chambers. Data were obtained from a representative experiment. (D) Lactate accumulates in the internal chamber of the culture system. Error bars represent SD from the mean obtained in two triplicated experiments.

(46) as a reporter for oxygen limitation. We used two experimental controls. First, we produced a similar culture system but without the separation between the two chambers. Under these conditions, diffusible substances can diffuse freely to and from the bulk above the cells, and therefore no horizontal gradients should be formed. Second, we modified our graded assay by separating the two chambers with a gas-permeable membrane of polydimethylsiloxane (PDMS). In this setting, certain diffusibles such as glucose and lactate will not permeate through the membrane. However, oxygen and other gases can diffuse freely (47). As expected, no GFP was detected in either of the control settings, and cells maintained their viability, confirming that oxygen permeates PDMS freely. In contrast, in the glass-separated chamber, GFP levels increased significantly in a manner dependent on the distance from the slit, showing evidence of oxygen limitation (Fig. 3C and *SI Appendix*, Fig. S5B). Hence, our system allows the spontaneous formation of oxygen gradients due to its diffusion into the internal chamber antagonized by cell consumption, similar to the process in actual tumors (42).

We next asked whether waste products, and lactic acid in particular, accumulate within our assay. We measured the levels of relevant metabolites in the internal chamber and in the external chamber (Fig. 3D). Most measured metabolites did not show significant changes. However, the levels of lactate in the small internal chamber were more than fourfold higher than those in the external chamber (Fig. 3D; note that these are average values, and thus levels in ischemic regions are expected to be even higher). Visual inspection of any cell culture in our graded microenvironment chamber clearly reveals that pH gradients are formed because phenol red in the media gains a yellow hue in the deep interior regions, indicating low pH, while it retains its pink color near the slit. To assess this more rigorously, we measured spatial gradients of pH directly using BCECF, a widely used fluorescent ratiometric pH probe. After only 2 d of culture, clear pH gradients emerged in our graded microenvironment chamber (*SI Appendix*, Fig. S6). Taken together, these data show that the *in vitro* cellular system adequately models the gradients of resources, the accumulation of waste products, and the pH gradients that occur within tumors.

**Emergence of Spatial Structure in Tumor/Macrophage Cocultures.** We cocultured MTLn3 cells and macrophages using our graded microenvironment system. Typically, an  $\sim 10^5$  cell homogenous

mix of macrophages and MTLn3 cells at a 1:1 ratio was seeded. As expected, in cocultures with no gradients both cell types remained evenly distributed during the entire experiment (1 wk) (Fig. 4A). In sharp contrast, when diffusion was limited by the glass cover, spatial structure emerged in the cell population after a similar time (Fig. 4B). In well-perfused regions close to the slit, macrophages coexist with MTLn3 cells. However, in distal regions, the number of macrophages drops significantly relative to MTLn3 (Fig. 4B,  $P < 0.0001$ ). Using the position of macrophages, we calculated macrophage density as a function of the distance from the slit (*SI Appendix*, Fig. S7A and B). We found that macrophage density drops  $\sim 10$ -fold in ischemic regions (*SI Appendix*, Fig. S7C). Although macrophages are affected the most, metabolic gradients additionally affect MTLn3 cells as their density also drops. In fact, high-cell-density clumps are visible in the culture without cover whereas in the graded condition there is high cell density only near the slit (Fig. 4A). We conducted the same experiment with two alternative cancer cell lines, H1650 or MDA-MB-231, also in coculture with macrophages. The experiments showed similar emergence of spatial structure (*SI Appendix*, Fig. S8A).

Our computational model predicts that lactic-acid-induced patterns occur even when glucose, and other nutrients, are not limiting. If this is correct, cocultures under nutrient gradients, but with uniformly low-lactic-acid levels, should not display spatial structure. To test this, we used a PDMS separation between the two chambers that, because of its oxygen permeability, will diminish lactic acid production (Fig. 1A). No spatial structure emerged under these conditions (*SI Appendix*, Fig. S7C), supporting that the hypoxic boost in lactic acid production is required for the emergence of spatial structure. Because macrophages are not directly affected by hypoxia (*SI Appendix*, Fig. S24) but hypoxia can lead to high levels of lactic acid that are lethal for macrophages (Fig. 1B and C), we conclude that metabolic alterations of the microenvironment cause macrophage death and the spontaneous emergence of tumor spatial structure.

**Macrophage Death Due to Glycolytic Metabolism.** Macrophages also produce lactic acid, especially under hypoxia, but they do so at a much lower level than MTLn3 cells (five- to eightfold lower levels, Fig. 1A). Accordingly, macrophages cultured alone at the same initial density showed little or no spatial structure (*SI Appendix*, Fig. S8B). However, in theory, higher numbers of

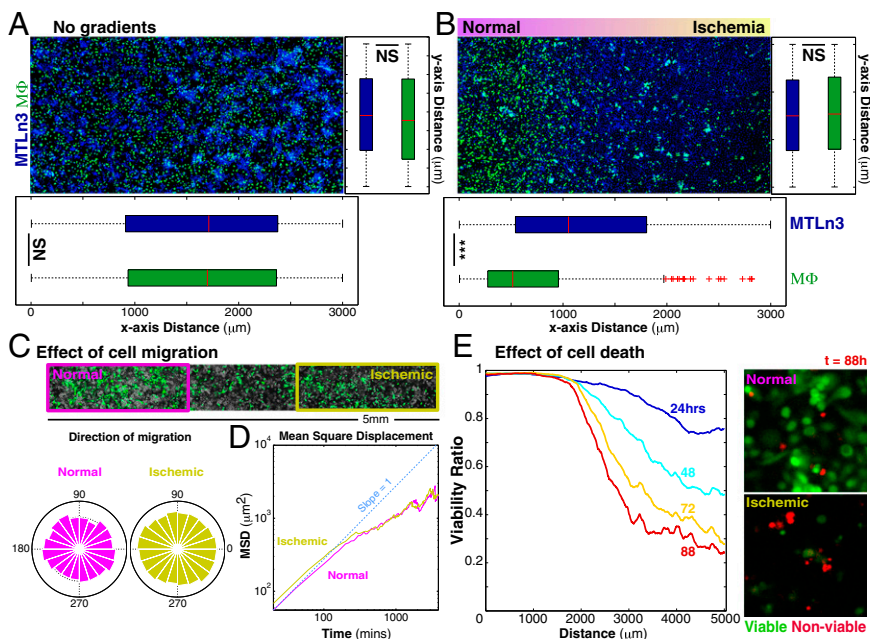


**Fig. 4.** Emergence of spatial structure in tumor/macrophage cocultures. (A) Cocultures with no gradients show no spatial structure as the distribution of macrophages (MΦ, labeled in green with CD68) and cancer cells is not significantly different (boxplots). (B) Spatial structure emerges when cocultures are performed in the culture system that mimics the tumor microenvironment. (C and D) Effect of cell migration (slope = 1). (E) Percentage of nonviable macrophages increases over time and with the distance from opening. (Right) Representative visual fields. Macrophages are in green, and nonviable macrophages are in red.  $***P < 0.001$ ; NS, not significant. Data were obtained from representative cases. Experiments were repeated at least two times.

macrophages should produce enough lactate to reproduce the localization patterns. We therefore repeated the experiment, but this time seeding  $\sim 10^6$  macrophages (10 $\times$  the previous cell density), and we were able to generate spatial structure in macrophage monocultures (SI Appendix, Fig. S8B). Macrophage disappearance was so extreme that virtually no macrophages could be found in ischemic regions (SI Appendix, Fig. S8C). These data support the conclusion that the spatial structure observed in cocultures is not caused by cancer cells specifically, but rather by the accumulation of metabolic waste products.

The patterns in our model can be explained by cell death (Fig. 2D). An alternative mechanism is that cells migrate from ischemic to well-perfused regions. To test this, we performed time-lapse imaging on cocultures within the graded microenvironment assay. We took advantage of the combination of high resolution and the wide field of tiling microscopy to track individual macrophages over a large area ( $\sim 5.4 \times 0.65$  mm). For quantitative analyses, we defined two regions of interest: the region comprising the first 2 mm proximal to the slit was designated as “Normal,” and the distal 2 mm of the image was designated as “Ischemic” (Fig. 4C). Initially the two cell types were distributed along the entire area but, after 72 h, macrophages were practically absent from the ischemic region (SI Appendix, Movie S2). More than 700 trajectories were analyzed. Only small but statistically significant differences in speed and persistence of normal versus ischemic macrophages were found (SI Appendix, Fig. S9A and B). Nevertheless, there was no significant preference in the direction of migration that could explain the spatial structure observed in our experiments (Fig. 4C). More formally, the mean square displacement of either macrophage group was diffusive or subdiffusive, revealing no directional bias toward the slit (Fig. 4D). The calculated diffusivity constant for these cells was less than  $2 \mu\text{m}^2/\text{min}$  ( $1.7 \pm 0.2 \mu\text{m}^2/\text{min}$  in the highest case), which means that the cells would require times on the order of months to travel the distances in the millimeter scale required to explain the patterns. Thus, the role of cell migration in determining this spatial structure is negligible.

It is possible, then, that ischemic macrophages undergo a metabolic collapse due to high lactic acid, low glucose, hypoxia, etc. In fact, careful examination of the later frames in the time-lapse imaging movie shows that ischemic macrophages indeed slow down their movements, round up, and eventually disappear (SI Appendix, Movie S2). Cells typically round up in shape before dying (48). Accordingly, calculation of cell circularity shows that macrophages distal to the slit tend to be more circular than proximal ones (SI Appendix, Fig. S9C). To examine cell death more closely, we performed a time-lapse of a high-density macrophage culture with propidium iodide (PI) in the media to label nonviable cells (SI Appendix, Movie S3); PI is more adequate for time-lapse experiments (SI Appendix). As shown in Fig. 4E, the proportion of nonviable macrophages significantly increases over time but only for macrophages distant from the slit. Together, these results show that cell death, not migration, drives pattern formation because ischemic regions of the gradient assay are more toxic for macrophages than for MTLn3 cancer cells.

**Role of Macrophage Recruitment in Spatial Structure.** Our measurements show that macrophage motility does not play a role in the emergence of spatial structure in the *in vitro* graded microenvironment. *In vivo*, however, macrophages can be activated and recruited to a tumor (22, 23, 32–34), and this active recruitment is likely to have an important role in TAM spatial structure. To test the role of TAM recruitment on spatial organization, we conducted 2D simulations of an expanding tumor with and without macrophage recruitment. We adapted the computational model to simulate an expanding tumor mass surrounded by well-irrigated stroma (SI Appendix, Fig. S10A) and simulated several scenarios by varying (i) the presence of macrophages in the initial tumor, (ii) the recruitment of macrophages to the tumor, and (iii) different values for the relative sensitivity of cancer cells and macrophages to an acidic environment. The

simulations showed that macrophage recruitment can lead to spatial structure, but macrophage sensitivity to an ischemic environment can greatly enhance the effect (SI Appendix, Fig. S10 and Movie S4). To test the role of macrophage recruitment further, we conducted additional chamber experiments where macrophages were introduced in the chamber only after 48 h. Consistent with our model, macrophages could not colonize deep regions within the system (SI Appendix, Fig. S11), supporting that the ischemic environment plays a key role in spatial patterning even when macrophages arrive in the system at later stages of tumor development.

## Discussion

Mathematical models of cancer have been developed for more than half a century, but only recently have oncologists recognized their value (49). Here we used a combination of mathematical modeling and *in vitro* experiment to show that cell metabolism can spontaneously create spatial heterogeneity in the extracellular milieu when perfusion is limited. Low-grade early tumors typically have TAMs, but these are homogeneously spread throughout the tumor, showing no evident spatial structure. Spatial structure where TAMs are enriched at the edge of tumors is evident only in later, possibly more ischemic, tumors (SI Appendix, Fig. S4) (30). Our model provides a mechanistic explanation for these observations, suggesting that microenvironmental heterogeneities are key to establishing spatial patterns of localization of tumor-associated macrophages.

In addition to being at the edge of large tumors, TAMs can also be found in necrotic/anoxic regions from where they are proposed to promote angiogenesis (28). This is consistent with our experiments, as hypoxia *per se* does not kill macrophages (SI Appendix, Fig. S2A). Hypoxia and pH levels in tumors are not always correlated (15). Thus, we expect that TAMs in the necrotic core could survive in regions that, despite being hypoxic, have lower levels of lactic acid (50). Accordingly, in our experiments we have observed that macrophages can survive in hypoxic regions where there are fewer cancer cells.

Our model does not rule out additional mechanisms for spatial patterning of TAMs (22, 23, 32–34). Macrophages can infiltrate through tissues via para- or transcellular migration (51). However, it is not clear why infiltrating macrophages do not adopt a homogeneous distribution within tumors. Our results suggest one explanation: the same microenvironment that is lethal for macrophages in our culture should prevent infiltrating macrophages from colonizing deep regions of the tumor. Thus, the effect of metabolic alterations on the tumor microenvironment may synergize with other known mechanisms of macrophage localization.

We investigated spatial structuring of TAMs, which typically constitute the most prominent stromal cell population in tumors and often promote tumor progression (23, 24, 52, 53). Clinical evidence shows that the colocalization of carcinoma cells and macrophages near capillaries is correlated with metastasis in breast cancer (54). Thus, spatial structure may be a key element in tumor-promoting activities of TAMs. For example, localized invasion and entry of cancer cells into the bloodstream may be more effective when macrophages are not evenly distributed. Nonetheless, the metabolically altered microenvironments can have effects on stromal cells other than TAMs and, thus, may be a general mechanism for the emergence of spatial structure. For example, human cytotoxic T lymphocytes infiltrating lactic-acid-producing multicellular tumor spheroids have reduced cytokine production and proliferation, and low pH induces anergy (55, 56).

The intimate link between metabolism and intracellular processes, such as cell-signaling cascades and gene regulation, has revitalized tumor metabolism research (2–9). However, most studies focus on the intracellular mechanisms, and little attention has been paid to the extracellular consequences of cancer metabolism. We show here that tumor metabolic alterations can have a considerable impact on their microenvironment, leading to alterations of tumor-stromal spatial structure. If shown to be widespread, the modulation of cell metabolism and the extracellular

milieu composition may open therapeutic possibilities. At the same time, they may force a rethinking of the microenvironmental consequences of current therapeutic strategies. For example, because ischemic regions can favor the emergent-resistant and aggressive clones (57, 58), therapies that target processes such as angiogenesis can lead to more and larger ischemic regions and potentially select for cancer lineages that are fitter than stromal cells.

## Methods

Extraction and differentiation of BMDMs were performed according standard protocols (30). The graded microenvironment assay was created from glass-bottom glass dishes (Matek) based on a tissue mimetic assay

(45). Microscopy was performed using an AxioObserver.Z1 (Zeiss), and images were analyzed with custom-made scripts in Matlab (MathWorks). For modeling details and complete methodology, please refer to [SI Appendix](#).

**ACKNOWLEDGMENTS.** We thank Catherine Konopacki, Inna Serganova, Grégoire Altan-Bonnet, Chris Sander, and the J.B.X. laboratory for helpful discussions and critical reading. We thank Inna Serganova for C6-HRE-GFP cells, Jeffrey Segall for MTLn3 cells, the Memorial Sloan-Kettering Cancer Center (MSKCC) metabolomics core facility for aid in measuring metabolites, and Joana Alves Vidigal for help in obtaining fresh MEFs. This work was supported by National Cancer Institute Grant CA148967 (to J.B.X. and J.A.J.) through the Integrative Cancer Biology Program and by the Office of the Director, National Institutes of Health, under Award DP2OD008440 (to J.B.X.). C.C.-F. is a Center for Cancer System Biology Independent Fellow. L.A. is supported by a MSKCC Brain Tumor Center fellowship.

- Warburg O (1956) On the origin of cancer cells. *Science* 123(3191):309–314.
- Gatenby RA, Gillies RJ (2004) Why do cancers have high aerobic glycolysis? *Nat Rev Cancer* 4(11):891–899.
- DeBerardinis RJ, Lum JJ, Hatzivassiliou G, Thompson CB (2008) The biology of cancer: Metabolic reprogramming fuels cell growth and proliferation. *Cell Metab* 7(1):11–20.
- Vander Heiden MG, Cantley LC, Thompson CB (2009) Understanding the Warburg effect: The metabolic requirements of cell proliferation. *Science* 324(5930):1029–1033.
- Koppenol WH, Bounds PL, Dang CV (2011) Otto Warburg's contributions to current concepts of cancer metabolism. *Nat Rev Cancer* 11(5):325–337.
- Cairns RA, Harris IS, Mak TW (2011) Regulation of cancer cell metabolism. *Nat Rev Cancer* 11(2):85–95.
- Lunt SY, Vander Heiden MG (2011) Aerobic glycolysis: Meeting the metabolic requirements of cell proliferation. *Annu Rev Cell Dev Biol* 27:441–464.
- Wellen KE, Thompson CB (2012) A two-way street: Reciprocal regulation of metabolism and signalling. *Nat Rev Mol Cell Biol* 13(4):270–276.
- Ward PS, Thompson CB (2012) Metabolic reprogramming: A cancer hallmark even Warburg did not anticipate. *Cancer Cell* 21(3):297–308.
- San Martín A, et al. (2013) A genetically encoded FRET lactate sensor and its use to detect the Warburg effect in single cancer cells. *PLoS ONE* 8(2):e57712.
- Zhang J, Nuebel E, Daley GQ, Koehler CM, Teitell MA (2012) Metabolic regulation in pluripotent stem cells during reprogramming and self-renewal. *Cell Stem Cell* 11(5):589–595.
- Wang R, et al. (2011) The transcription factor Myc controls metabolic reprogramming upon T lymphocyte activation. *Immunity* 35(6):871–882.
- Mazurek S, Boschek CB, Hugo F, Eigenbrodt E (2005) Pyruvate kinase type M2 and its role in tumor growth and spreading. *Semin Cancer Biol* 15(4):300–308.
- Lee EY, et al. (2009) Hypoxia-enhanced wound-healing function of adipose-derived stem cells: Increase in stem cell proliferation and up-regulation of VEGF and bFGF. *Wound Repair Regen* 17(4):540–547.
- Helmlinger G, Yuan F, Dellian M, Jain RK (1997) Interstitial pH and pO<sub>2</sub> gradients in solid tumors in vivo: High-resolution measurements reveal a lack of correlation. *Nat Med* 3(2):177–182.
- Gatenby RA, et al. (2007) Cellular adaptations to hypoxia and acidosis during somatic evolution of breast cancer. *Br J Cancer* 97(5):646–653.
- Nowell PC (1976) The clonal evolution of tumor cell populations. *Science* 194(4260):23–28.
- Merlo LM, Pepper JW, Reid BJ, Maley CC (2006) Cancer as an evolutionary and ecological process. *Nat Rev Cancer* 6(12):924–935.
- Gatenby RA, Gawlinski ET (1996) A reaction-diffusion model of cancer invasion. *Cancer Res* 56(24):5745–5753.
- Anderson AR, Weaver AM, Cummings PT, Quaranta V (2006) Tumor morphology and phenotypic evolution driven by selective pressure from the microenvironment. *Cell* 127(5):905–915.
- Gatenby RA, Gillies RJ (2008) A microenvironmental model of carcinogenesis. *Nat Rev Cancer* 8(1):56–61.
- Mantovani A, Allavena P, Sica A, Balkwill F (2008) Cancer-related inflammation. *Nature* 454(7203):436–444.
- Joyce JA, Pollard JW (2009) Microenvironmental regulation of metastasis. *Nat Rev Cancer* 9(4):239–252.
- Qian BZ, Pollard JW (2010) Macrophage diversity enhances tumor progression and metastasis. *Cell* 141(1):39–51.
- Bingle L, Brown NJ, Lewis CE (2002) The role of tumour-associated macrophages in tumour progression: Implications for new anticancer therapies. *J Pathol* 196(3):254–265.
- Zhang QW, et al. (2012) Prognostic significance of tumor-associated macrophages in solid tumor: A meta-analysis of the literature. *PLoS ONE* 7(12):e50946.
- Cramer T, et al. (2003) HIF-1 $\alpha$  is essential for myeloid cell-mediated inflammation. *Cell* 112(5):645–657.
- Murdoch C, Giannoudis A, Lewis CE (2004) Mechanisms regulating the recruitment of macrophages into hypoxic areas of tumors and other ischemic tissues. *Blood* 104(8):2224–2234.
- White C, et al. (2009) Copper transport into the secretory pathway is regulated by oxygen in macrophages. *J Cell Sci* 122(Pt 9):1315–1321.
- Gocheva V, et al. (2010) IL-4 induces cathepsin protease activity in tumor-associated macrophages to promote cancer growth and invasion. *Genes Dev* 24(3):241–255.
- Wyckoff JB, et al. (2007) Direct visualization of macrophage-assisted tumor cell intravasation in mammary tumors. *Cancer Res* 67(6):2649–2656.
- Ren G, et al. (2012) CCR2-dependent recruitment of macrophages by tumor-educated mesenchymal stromal cells promotes tumor development and is mimicked by TNF $\alpha$ . *Cell Stem Cell* 11(6):812–824.
- Gil-Bernabé AM, et al. (2012) Recruitment of monocytes/macrophages by tissue factor-mediated coagulation is essential for metastatic cell survival and premetastatic niche establishment in mice. *Blood* 119(13):3164–3175.
- Ahn GO, et al. (2010) Inhibition of Mac-1 (CD11b/CD18) enhances tumor response to radiation by reducing myeloid cell recruitment. *Proc Natl Acad Sci USA* 107(18):8363–8368.
- Goswami S, et al. (2005) Macrophages promote the invasion of breast carcinoma cells via a colony-stimulating factor-1/epidermal growth factor paracrine loop. *Cancer Res* 65(12):5278–5283.
- DeBerardinis RJ, et al. (2007) Beyond aerobic glycolysis: Transformed cells can engage in glutamine metabolism that exceeds the requirement for protein and nucleotide synthesis. *Proc Natl Acad Sci USA* 104(49):19345–19350.
- Brizel DM, et al. (2001) Elevated tumor lactate concentrations predict for an increased risk of metastases in head-and-neck cancer. *Int J Radiat Oncol Biol Phys* 51(2):349–353.
- Walenta S, et al. (2000) High lactate levels predict likelihood of metastases, tumor recurrence, and restricted patient survival in human cervical cancers. *Cancer Res* 60(4):916–921.
- Xavier JB, Picioreanu C, van Loosdrecht MCM (2005) A framework for multidimensional modelling of activity and structure of multispecies biofilms. *Environ Microbiol* 7(8):1085–1103.
- Nadell CD, Foster KR, Xavier JB (2010) Emergence of spatial structure in cell groups and the evolution of cooperation. *PLoS Comput Biol* 6(3):e1000716.
- Peirce SM, Van Gieson EJ, Skalak TC (2004) Multicellular simulation predicts microvascular patterning and in silico tissue assembly. *FASEB J* 18(6):731–733.
- Thomlinson RH, Gray LH (1955) The histological structure of some human lung cancers and the possible implications for radiotherapy. *Br J Cancer* 9(4):539–549.
- Swanson KR, et al. (2011) Quantifying the role of angiogenesis in malignant progression of gliomas: In silico modeling integrates imaging and histology. *Cancer Res* 71(24):7366–7375.
- Hawkins-Daarud A, Rockne RC, Anderson ARA, Swanson KR (2013) Modeling tumor-associated edema in gliomas during anti-angiogenic therapy and its impact on imageable tumor. *Front Oncol* 3:66.
- Cochran DM, Fukumura D, Ancukiewicz M, Carmeliet P, Jain RK (2006) Evolution of oxygen and glucose concentration profiles in a tissue-mimetic culture system of embryonic stem cells. *Ann Biomed Eng* 34(8):1247–1258.
- Brader P, et al. (2007) Imaging of hypoxia-driven gene expression in an orthotopic liver tumor model. *Mol Cancer Ther* 6(11):2900–2908.
- Cox ME, Dunn B (1986) Oxygen diffusion in poly(dimethyl siloxane) using fluorescence quenching. I. Measurement technique and analysis. *J Polym Sci A Polym Chem* 24:621–636.
- Rello S, et al. (2005) Morphological criteria to distinguish cell death induced by apoptotic and necrotic treatments. *Apoptosis* 10(1):201–208.
- Rejniak KA, Anderson ARA (2012) State of the art in computational modelling of cancer. *Math Med Biol* 29(1):1–2.
- Serganova I, et al. (2011) Metabolic imaging: A link between lactate dehydrogenase A, lactate, and tumor phenotype. *Clin Cancer Res* 17(19):6250–6261.
- Ley K, Laudanna C, Cybulsky MI, Nourshargh S (2007) Getting to the site of inflammation: The leukocyte adhesion cascade updated. *Nat Rev Immunol* 7(9):678–689.
- Mantovani A, Bottazzi B, Colotta F, Sozzani S, Ruco L (1992) The origin and function of tumor-associated macrophages. *Immunol Today* 13(7):265–270.
- Hanahan D, Coussens LM (2012) Accessories to the crime: Functions of cells recruited to the tumor microenvironment. *Cancer Cell* 21(3):309–322.
- Robinson BD, et al. (2009) Tumor microenvironment of metastasis in human breast carcinoma: A potential prognostic marker linked to hematogenous dissemination. *Clin Cancer Res* 15(7):2433–2441.
- Fischer K, et al. (2007) Inhibitory effect of tumor cell-derived lactic acid on human T cells. *Blood* 109(9):3812–3819.
- Calcinotto A, et al. (2012) Modulation of microenvironment acidity reverses anergy in human and murine tumor-infiltrating T lymphocytes. *Cancer Res* 72(11):2746–2756.
- Pàez-Ribes M, et al. (2009) Antiangiogenic therapy elicits malignant progression of tumors to increased local invasion and distant metastasis. *Cancer Cell* 15(3):220–231.
- Ebos JML, et al. (2009) Accelerated metastasis after short-term treatment with a potent inhibitor of tumor angiogenesis. *Cancer Cell* 15(3):232–239.